THE EFFECTS OF IMIPRAMINE BLUE ON VASCULAR PERMEABILITY IN GLIOBLASTOMAS

A Thesis
Presented to
The Academic Faculty

by

Eleanor DeHitta

In Partial Fulfillment
of the Requirements for the
Undergraduate Research Option Certificate in the
School of Biomedical Engineering, College of Engineering

Georgia Institute of Technology
May 6, 2011

THE EFFECTS OF IMIPRAMINE BLUE ON VASCULAR PERMEABILITY IN GLIOBLASTOMAS

Approved by:

Dr. Ravi Bellamkonda, Advisor
School of Biomedical Engineering
Georgia Institute of Technology

Dr. Brandon Dixon
School of Mechanical Engineering
Georgia Institute of Technology

Dr. Paul Benkeser
School of Biomedical Engineering
Georgia Institute of Technology

Date Approved: May 6, 2011

ACKNOWLEDGEMENTS

I would like to thank my faculty advisor Dr. Ravi Bellamkonda for providing me an opportunity to participate in undergraduate research and reinforcing my scientific inquiry with the perpetual "Why?" question. Additionally, I would like to thank my second advisor, Dr. Brandon Dixon for his guidance and support.

I would like to thank my research mentor Jennifer "Jenny" Munson for infecting me with her contagious love for research and constant assistance even while living 5,000 miles away. Thank you to Dr. Kathleen McKneeley and Alexander Ortiz for their mentorship and aid while Jenny was away. Furthermore, this research would not have been accomplished without my loving liposome lab family: Mona Ahmad, Sydney Rowson, Rania Khan, Shalini Nemani, Cong Guo, Choyce Middleton, Anna Olsen, and Benjamin Roller. Their laughter and support were essential to the completion of my thesis.

TABLE OF CONTENTS

ACKNOWLEDGEMENTS 1
TABLE OF CONTENTS 2
LIST OF TABLES 4
LIST OF FIGURES 5
LIST OF SYMBOLS AND ABBREVIATIONS 6
SUMMARY 7
1. INTRODUCTION 9
1.1. GLIOMAS AND THEIR CHARACTERISTICS 9
1.2. ANGIOGENESIS IN GLIOMAS 9
1.3. TREATMENTS FOR GLIOMAS 10
2. LITERATURE REVIEW 11
2.1. NANOTHERAPEUTICS 11
2.2. LIPOSOMES 12
2.3. LIPOSOMAL CONTRAST AGENTS 14
2.4. IMIPRAMINE BLUE 15
3. MATERIALS AND METHODS 17
3.1. MATERIALS 17
3.1.1. CELL CULTURE MATERIALS 17
3.1.2. CELL LINES 17
3.1.3. IMIPRAMINE BLUE AND LIPOSOME MATERIALS 18
3.1.4. ANIMAL STUDY MATERIALS 19
3.2.1. MATRIX METALLOPROTEINASES ASSAY 19
3.2.2. ENDOTHELIAL CELL INVASION ASSAY 20
3.3. *IN VIVO* VASCULAR PERMEABILITY QUANTIFICATION 21
3.3.1. IMIPRAMINE BLUE LIPOSOME FORMULATION 21
3.3.2. PLAIN LIPOSOME FORMULATION 22
3.3.3. DUAL GADOLINIUM LIPOSOME FORMULATION 22
3.3.4. 3RT1-RT2A GLIOMA CELL CULTURE 23
3.3.6. TAIL VEIN INJECTIONS 23
3.3.7. MAGNETIC RESONANCE IMAGING 24
3.3.8. IMAGE AND DATA ANALYSIS 24

3.3.8.1. KINETIC ANALYSIS 24
3.3.8.2. MRI DATA EXTRACTION 25
3.3.9. PERFUSIONS AND BRAIN PROCESSING..... 28
4. RESULTS 28
4.1. IN VITRO 28
4.1.1. MMP ACTIVITY..... 28
4.1.2. HUVEC INVASION 31
4.2. *IN VIVO* VASCULAR PERMEABILITY QUANTIFICATION 31
5. DISCUSSION 32
7. REFERENCES..... 38
8. ADDENDUM..... 40

LIST OF TABLES

Table	Title	Page
1	Vascular Permeability Study Timeline	21
2	Endothelial Transfer Coefficients (KPS) and Cross-Sectional Tumor Areas in Plain Liposome-Treated and Imipramine Blue Liposome-Treated 3RT1-RT2A Tumors.	32

LIST OF FIGURES

Figure	Title	Page
1	Liposome Schematic	13
2	Nanoparticles Delivered to Tumor via EPR Effect	14
3	Effects of Imipramine Blue in Rat Glioma (3RT1-RT2A) Model.	16
4	Doxorubicin concentration in plasma of rats treated with liposome-encapsulated doxorubicin.	27
5	Predicted gadolinium concentration in plasma of rats treated with dual-gadolinium liposomes.	27
6	MMP Activity in IB-Treated U87 Cells	29
7	MMP Activity in IB-Treated RT2A cells.	30
8	Invasion of IB-Treated HUVECs.	31
9	$1/T_1$ MR Brain Image Colormaps.	32
10	Effects of Imipramine Blue on Blood Vessels of Rat Gliomas (3RT1-RT2A).	35

LIST OF SYMBOLS AND ABBREVIATIONS

BME	Basement membrane extract
C_p	Concentratino of gadolinium in plasma
CT	Computerized Tomography
C_t	Concentration of gadolinium in tumor
C_t	Concentration of gadolinium in tumor
DAPI	4',6-Diamidino-2-phenylindole
DMEM	Dulbecco's Modified Eagle's Medium
DPPC	1,2-dipalmitoyl-*sn*-glycero-3-phosphocholine
DSPC	Distearoyl (sn-glycero) phosphotidylcholine
EPR	Enhanced permeability retention
FITC	Fluorescein isothiocyanate
f_{pv}	Fractional plasma volume
GBM	Glioblastoma Multiforme
Gd	Gadolinium
GFP	Green fluorescent protein
IACUC	Institutional Animal Care and Use Committee
IB	Imipramine Blue
K^{PS}	Endothelial transfer coefficient
M199	Medium 199
MMP	Matrix metalloproteinase
MRI	Magnetic resonance imaging
OCT	Optimal cutting temperature compound
PBS	Phosphate buffered saline
PEG	Polyethylene glycol
RECA-1	Rat endothelial cell antibody 1
RES	Reticuloendothelial system
RGB	Red, green, blue
TE	Echo time
TR	Repetition time

SUMMARY

Glioblastoma (GBM), a form of glioma, is an aggressive form of human cancer with a median survival time of 14.6 months with after diagnosis. It is the most common and most aggressive form of brain cancer due to its invasive and angiogenic nature. Gliomas develop their vascularized networks through the process of angiogenesis, the development of blood vessels. In tumor development, angiogenesis is marked by a few hallmark characteristics: degradation of the basement membrane, recruitment of endothelial cells, and tube network formation among recently recruited endothelial cells to finalize the formation of a new blood vessel. Angiogenesis increases vascular permeability of blood vessels, which can ultimately progress from edema, to neurological deficits, to death. Anti-angiogenic therapies have been favored for reducing symptoms related with edema. Imipramine Blue (IB) is a novel compound used to treat gliomas. *In vivo*, it decreases invasion and prolongs survival. It is believed that IB's ability to stop tumor cells from invading into neighboring areas also inhibits angiogenesis. If the tumor cells cannot move to create more blood vessels, then angiogenesis might also be inhibited. Additionally, it is believed that IB might stop the recruitment of endothelial cells, similar to how IB stops tumor cell invasion. This study investigated Imipramine Blue's possible anti-angiogenic effects.

In vitro, IB did not affect MMP-2 and MMP-9 activity in U87 and RT2A glioma cell lines (ANOVA). IB did not affect HUVEC invasion ($p=0.08$, two-pair, student's t-test, $\alpha=0.05$). *In vivo,* animals were treated with IB liposomes or plain liposomes, and vascular permeability was assessed using kinetic image analysis from MRI with the aid of contrast-enhancing dual-gadolinium liposomes. This method is useful for animal

studies that want to investigate different variables from the same brain. No significant differences in endothelial transfer coefficients (K^{PS}) were observed between treatment groups (two-sample student's t-test, $p = 0.3488$), suggesting IB does not affect vascular permeability. *In vitro* and *in vivo* results suggest that IB does not have anti-angiogenic effects.

1. INTRODUCTION

1.1. GLIOMAS AND THEIR CHARACTERISTICS

Glioblastoma (GBM), a form of glioma, is an aggressive form of human cancer with a median survival time of 14.6 months with treatment (surgery, radiation, and chemotherapy) after diagnosis.[1] It is the most common and most aggressive form of brain cancer.[2] GBM's tumor originally arises from the glial cells of the brain. Like any form of cancer, GBM has the potential of invading neighboring tissue (invasion), but what separates gliomas from other forms of cancer is the primary organ in which it originates. The brain is the central controlling unit of the body. Tumor growth can create intracranial pressure, forcing the tissue to shift, resulting in eventually death due to stroke (disturbance of blood flow in the brain) or cerebral edema (excess accumulation of water in the brain).[3]

1.2. ANGIOGENESIS IN GLIOMAS

Gliomas develop their vascularized networks through the process of angiogenesis, the development of blood vessels. In tumor development, angiogenesis is marked by a few hallmark characteristics. Growth factors released from tumor cells activate receptors on nearby pre-existing blood vessels, causing the release of enzymes called matrix metalloproteases (MMPs).[4] Matrix metalloproteases degrade the basement membrane or inner lining of the blood vessel to make room for the development of new blood vessels. In gliomas, MMP-2 and MMP-9 are significantly overexpressed.[5] Simultaneously, the blood vessel's pre-existing endothelial cells release chemical messengers to induce endothelial cell recruitment towards the site of angiogenesis (known as endothelial cell chemotaxis). Blood vessels are mainly composed of endothelial cells. They are the building blocks of the blood vessel foundation. Endothelial cells will then adhere to the

site of degraded basement membrane. Next, the newly recruited endothelial cells will form tube-like structures with neighboring endothelial cells. These networks will facilitate the development of blood vessel formation.[4]

Throughout the process of angiogenesis, growth factors are overexpressed. An imbalance of these growth factors causes the newly formed vessels to be disorganized and underdeveloped[6]. The endothelial cells which make up the lining of the vessel have large gap junctions as a result of the imbalance in growth factors[7]. The creation of large gap junctions increases the permeability of the blood vessel, which causes fluid accumulation in tumors. Tumor permeability has been observed to increase up to 20 fold compared to healthy patients.[8] The blood-brain barrier is the separation between blood and cerebrospinal fluid. It is highly selective of deciding what can reach brain tissue. Gliomas disrupt the structure of the blood-brain barrier, allowing for unwanted fluid to accumulate. Fluid accumulation (edema) can increase interstitial fluid pressure and neurological deficits. Furthermore, interstitial fluid pressure has been shown to decrease drug delivery. Although edema can be treated with steroid therapy, it is not favored due to the adverse side effects associated with steroids. Therefore, development of anti-angiogenic therapies is favored to reduce symptoms of edema and increase drug delivery.[8]

1.3. TREATMENTS FOR GLIOMAS

The low chances of surviving GBM are associated with the invasive and highly vascularized nature of the tumor. Unfortunately, current treatments are mainly focused on alleviating symptoms (seizures, neurological deficits, psychological instabilities)

rather than finding a cure.[3] Treatments include surgery, radiotherapy, and chemotherapy. MRI (magnetic resonance imaging) and CT (computed tomography) can be used for initial detection of a tumor prior to surgery, but a biopsy analysis, extraction and analysis of the tumor cells, is the only way of determining the grade or malignancy of the tumor.[3] Removal of the tumor, or resection surgery is usually conducted to decrease symptoms and to obtain samples for diagnosis.[3] Unlike other forms of cancer, tumors in the brain are difficult to remove without neural complications arising. Removal of a tumor located in areas necessary for cognitive function could result in the inability of the patient to retain information or think as well as he or she could previously. Even after personalized therapy, tumors recur with a median survival of 25 weeks.[1] For this reason, it is essential to find more effective means of prolonging survival by targeting GBM's invasiveness and vasculature. The Bellamkonda Lab of Georgia Tech uses nanotherapeutics to target these characteristics.

2. LITERATURE REVIEW

2.1. NANOTHERAPEUTICS

Nanotechnology has been a thriving focal point of today's innovations because it can perform tasks on a molecular scale and possess a widespread of applications. Consequently, there has been a spike in funding for research in this field for cancer therapy because it has the potential of analyzing and stopping cancer on the molecular scale. For instance, the National Cancer Institute committed $144.3 million for their cancer-nanotherapy sector from 2005 to 2010.[7] To be considered nanotechnology, an object or material must be smaller than 100 nm in radius. The six most studied

nanoparticles are: nanoshells, carbon nanotubes, dendrimers, quantum dots, superparamagnetic nanoparticles, and liposomes.[7] They can be used for drug delivery, gene therapy, or imaging. Each type of nanoparticle takes advantage of the same general mechanisms of targeting cancer cells--recognizing and finding the tumor and delivering a load to the tumor cells (anti-cancer drugs, genes, or contrast-enhancing agents).[7]

2.2. LIPOSOMES

Of these nanoparticles, liposomes comprise a considerable amount of nanotechnology research in biomedicine. Liposomes are vesicles, like cells, but without organelles inside their aqueous center (Figure 1).[9] Liposomes with membranes composed of naturally occurring phospholipids and cholesterol are not used for drug delivery because they are easily detected, marked as a "foreigner", and removed by the reticuloendothelial system (RES).[10] Therefore the membranes are conjugated with molecules to inhibit the liposome from being marked as a "foreigner" and cleared from the blood. Polyethylene glycol (PEG) is a commonly used conjugate because it spatially blocks the liposome from being marked for plasma clearance (or removed from the body).[10] Studies have shown that PEG-conjugated liposomes yield a systemic plasma clearance 200-fold less than the non-PEG conjugated liposomes.[10] PEG has become a standard conjugate because it allows liposomes to circulate the body significantly longer than non-conjugated liposomes. Additionally, the size of the liposome is customized for delivery to the tumor.[6]

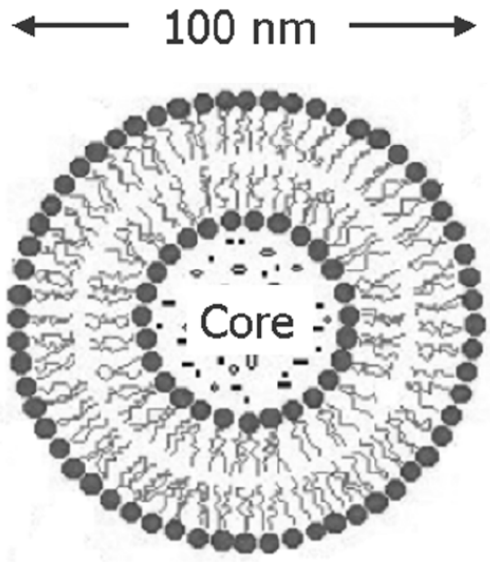

Figure 1: Liposome Schematic: Vesicle of about 100nm with a phospholipid bilayer and aqueous core.[11]

The size of the liposome also aids in avoiding RES clearance. RES clearance of liposomes occurs in the sinusoid of the spleen and the liver. Their filtration vessels range from 150 to 200 nm in diameter. Particles larger than the vessel diameter are retained in the organs and are isolated from the rest of the body. Liposomes less than 150 nm can be passed through the vessels and returned to the blood stream. As a result, combinations of lipids, conjugates, cholesterol, and drugs have been tailored to find favorable formulations with higher circulation times.

Liposomes enter tumors via the enhanced permeability and retention effect (EPR).[6] A growing tumor needs nutrients in order to survive, typically resulting in the rerouting and generation of new blood vessels (angiogenesis).[6, 12] This allows particles up to 400nm in diameter, like liposomes, to passively accumulate in the tumor (Figure 2).[7] In contrast, non-tumor sites do not experience passive liposome accumulation because liposomes cannot pass through their intact and developed endothelial linings.[7]

Recent studies have shown that liposomes can be loaded with chemotherapeutic drugs to increase circulation time, increase concentration delivered to the point of interest, and decrease toxicity effects to vital organs.[13] For example, doxorubicin, a common chemotherapeutic, has been delivered in clinical trials to gliomas with success at passively targeting the tumor.[14] In contrast, no anti-invasive drugs are currently on the market. Although, there is a necessity for them, since invasion is an underlying characteristic of death due to GBM.

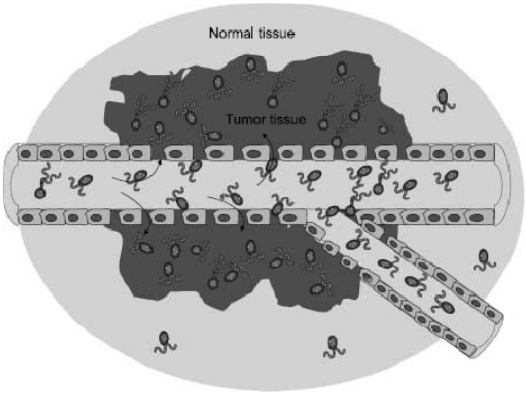

Figure 2: Nanoparticles delivered to tumor tissue via EPR Effect. The endothelial cells lining the blood vessel are more spaced out allowing nanoparticles of up to 400 nm in diameter to pass through and accumulate in a tumor.[6]

2.3. LIPOSOMAL CONTRAST AGENTS

T1-based magnetic resonance (MR) contrast agents have enabled more applications of magnetic resonance imaging (MRI) in tumor detection, tumor characterization, and vascular imaging. Gadolinium (Gd) chelates are ideal for imaging because they decrease T1 relaxation times.[15] However, bolus injection timing is important due to gadolinium's small window of efficacy and three hour half-life.[16] For *in vivo* small animal studies, Gd-chelates cannot produce a clear image with an optimized 7 T scanner.

Ghaghada *et al.* synthesized gadolinium liposomes: core encapsulated, surface conjugated, and dual (core encapsulated and surface conjugated) formulations. Three days after tail vein injections of the different formulations, animals were imaged. Rats which were administered the dual gadolinium formulation exhibited significantly higher nanoparticle-based T1 relaxivity, signal to noise ratio, and contrast to noise ratio, compared to rats with contrast-enhanced and surface conjugated gadolinium liposomes.[15]

2.4. IMIPRAMINE BLUE

In the Bellamkonda Lab at Georgia Tech, liposomes are being developed to stop invasion, clearly define the tumor for resection, and treat residual tumor cells left over from resectioning. Past projects have involved analyzing the effects of the novel drug, Imipramine Blue (IB), on a rat model of invasive glioma *in vivo*. Imipramine Blue is a drug developed by the Arbiser Lab of Emory University. It has poor solubility and circulation time in the bloodstream, so encapsulating the drug in a liposome is favorable to increase circulation in the body. This drug appears to limit invasion of tumor into healthy brain tissue but does not cause cytotoxic effects (i.e. induced cell death) in healthy tissue (Figure 3).

It is believed that IB's ability to stop tumor cells from invading into neighboring areas could also inhibit angiogenesis. If the tumor cells cannot move to create more blood vessels, then angiogenesis might also be inhibited. Additionally, it is believed that IB might stop the recruitment of endothelial cells, similar to how IB stops tumor cell invasion. Typically, rats inoculated with the untreated 3RT1-RT2A tumor model show signs of morbidity by day 12. Survival studies using the 3RT1-RT2A tumor model have shown that rats treated on day 4 with liposomal Imipramine Blue and day 7 with

liposomal doxorubicin (a chemotherapeutic agent) have delayed signs of morbidity from 12 days to 8 months, which is significantly greater than rats treated only with Imipramine Blue or doxorubicin. It is believed that Imipramine Blue possesses anti-angiogenic effects on vascular permeability, accounting for the prolongation of survival in rats treated with liposomal IB and doxorubicin

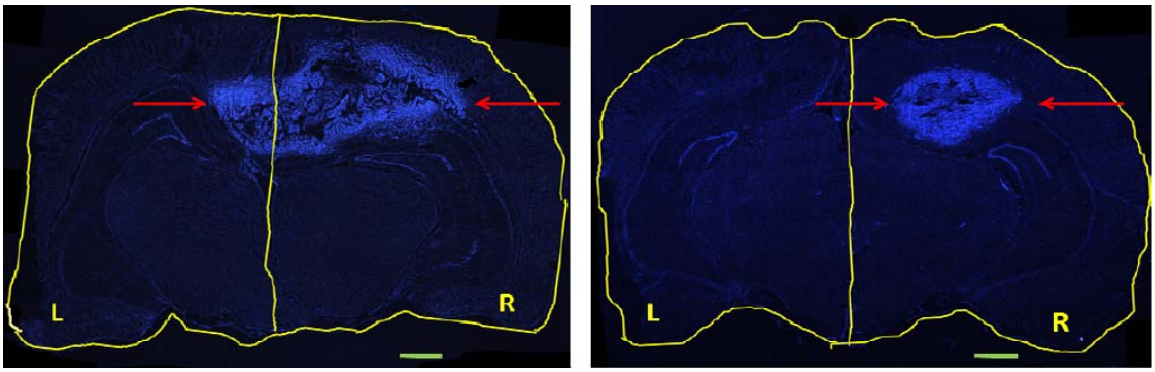

Figure 3: Effects of Imipramine Blue in Rat Glioma (3RT1-RT2A) Model. Tumors were injected 2mm anterior and lateral to lambda and 3 mm below the dura. Animals were administered tail-vein injections (saline or liposomal IB) on Day 4 and 7 (after tumor inoculation) and perfused on Day 11. Brains were sectioned coronally and stained with DAPI to highlight nuclei. The treated tumor appears more contained than the non-treated, suggesting IB's anti-invasive effects.[17]

3. MATERIALS AND METHODS

3.1. MATERIALS

3.1.1. CELL CULTURE MATERIALS

96-well plates (black-bottom), tissue-culture treated 96-well plates (clear) and T75 flasks were purchased from VWR (West Chester, PA). Trypsin-EDTA (0.05% trypsin, 0.53 mM EDTA) in Hanks' balanced salt solution was purchased from Mediatech (Manassas, VA). 5x basement membrane extract (BME) and 10x coating solution were purchased from Trevigen (Gaithersburg, MD). Dye-quenched (DQ) collagen (IV) and 4',6-Diamidino-2-phenylindole (DAPI) were purchased from Invitrogen. Transwells with 8 micron pore size were purchased from Millipore. Paraformaldehyde was purchased from Sigma (St. Louis, MO).

3.1.2. CELL LINES

U87MG human glioma cell line was purchased from American Type Culture Collection, (Manassas, VA) and grown in T-75 flasks in growth medium. U87MG growth medium consisted of Dulbecco's Modified Eagle's Medium (DMEM) supplemented with 10% Fetal Bovine Serum (FBS), 1% Penicillin/Streptomycin (P/S), 1% Non-Essential Amino Acids , and 1% L-glutamine (L-glut) (Gibco, Carlsbad, CA). RT2A and 3RT1-RT2A (eGFP-expressing RT2A) rat glioma cell lines were obtained from Helen Fillmore in the Department of Neurosurgery from the Virginia Commonwealth University. RT2A was grown in T-75 flasks in U87MG growth medium previously mentioned. 3RT1-RT2A growth medium included the same formulation for U87MG and RT2A growth medium with the addition of 1mg/ml G418 sulfate (Gemini Bio-Products, West Sacremento, CA). Basal media for

U87MG, RT2A, and 3RT1-RT2A consisted of DMEM supplemented with 1% Penicillin/Streptomycin, 1% Non-Essential Amino Acids , and 1% L-glutamine.

Human Umbilical Vein Endothelial Cells (HUVEC) were a generous gift from Larry V. McIntyre and cultured in T-75 flasks treated with 0.2% gelatin (Sigma, St. Louis, MO) in Medium 199 (M199, Mediatech, Manassas, VA) supplemented with 16.28% Fetal Bovine Serum, 0.98% Penicillin/Streptomycin, 0.98% L-glutamine, 0.2% heparin (1000 USP units ml−1, Baxter Healthcare, Deerfield, IL), and 0.16% endothelial mitogen (25 mg reconstituted in 2 ml M199, Biomedical Technologies, Stoughton, MA). Low serum media consisted of M199 supplemented with 0.05% Fetal Bovine Serum, 0.98% Penicillin/Streptomycin, 0.98% L-glutamine, 0.2% heparin, and 0.16% endothelial mitogen.

3.1.3. IMIPRAMINE BLUE AND LIPOSOME MATERIALS

Imipramine Blue was obtained from the Arbiser Laboratory of Emory University. Stock solutions for in vitro experiments diluted Imipramine Blue in ethanol. Distearoyl (sn-glycero) phosphotidylcholine (DSPC), poly (ethylene glycol) 2000-distearoyl-phosphatidyl ethanoloamine (DSPE-PEG 2000), 1,2-dipalmitoyl-*sn*-glycero-3-phosphocholine (DPPC), and Gd-DTPA bis(stearylamide) (Gd-DTPA-BSA) were purchased from Avanti (Alabaster, AL). Cholesterol was purchased from Sigma (St. Louis, MO). Gadolinium DTPA (Omniscan) and sepharose were purchased from GE Healthcare. Nuclepore extrusion filters of 0.4 μm 0.2 μm were purchased from Millipore. A 10 ml Lipex Thermoline extruder was purchased from Northern Lipids (Vancouver, BC).

3.1.4. ANIMAL STUDY MATERIALS

Fisher 344 rats (n=6) were purchased from Harlan (Indianapolis, IN). A stereotaxic frame was purchased from Kopf Instruments (Tujunga, CA). Marcaine (0.5%) was purchased from Abbott Laboratories (Abbott Park, IL). Isoflurane was purchased from Baxter Healthcare (Deerfield, IL). A 10 µl Hamilton syringe was purchased from Hamilton. Sutures (4-0) were purchased from Ethicon. Buprenorphine (0.05 mg/kg) was purchased from (Reckitt Benckiser). Nalgene syringe filters (0.2 µm) were purchased from Thermo Scientific (Rochester, NY). Ketamine (100 mg/ml) was purchased from Fort Dodge Laboratories (Madison, NJ). Xylazine (100 mg/ml) was purchased from The Butler company (Dublin, OH). Acetylpromazine (10 mg/ml) was obtained from Boehringer Ingelheim (Ingelheim, Germany). Optimal Cutting Temperature (OTC) Compound was purchased from VWR (Batavia, IL).

3.2. *IN VITRO* ANGIOGENESIS ASSAYS

3.2.1. MATRIX METALLOPROTEINASES ASSAY

U87MG human glioma cell line and RT2A rat glioma cell lines were cultured to confluence in growth medium. 5x BME was diluted to 1x in DMEM. Dye-quenched collagen (IV) was then diluted in the 1x BME solution to a final concentration of 1mg/ml. Dye-quenched collagen contains an excessive amount of fluorescein (fluorescent dye) attached to its structure.[18] The excessive amount of fluorescein decreases the spacing among neighboring fluorescein, resulting in almost no fluorescent signal emitted. When dye-quenched collagen is cleaved into fragments, a separation between the fluorescein is created, allowing for fluorescent emission. Emission of fluorescent signal indicates degradation of dye-quenched collagen by matrix metalloproteinases. The combination of

collagen IV and basement membrane extract simulate the basement membrane of the blood vessel.

A 96-well plate was coated with the dye-quenched collagen and BME solution and incubated at 37°C for 30 minutes. Wells were coated with glioma cell lines (50,000 cells/well, resuspended in 50 µl basal media) and treated with varying concentrations of Imipramine Blue (0 to 100 µM). Plates were then incubated for 16-24 hours and FITC imaged under 10x magnification. FITC intensity levels indicating MMP activity were observed using ImageJ. Average FITC intensity levels were recorded, normalized to the control (0µM), and compared using a one-way ANOVA to detect significant differences. If the one-way ANOVA detected a significant difference, a Tukey comparison was used to determine which pairs were significantly different

3.2.2. ENDOTHELIAL CELL INVASION ASSAY

A 10x coating solution was diluted to 1x in sterile water. A 5x BME solution was then diluted to 1x using the diluted 10x coating solution previously mentioned, creating the final BME coating solution. Transwells were placed in 24-well plates, coated with the BME coating solution, incubated at 37°C for 16-24 hours, and aspirated and washed with PBS. Transwells were then coated with cells (50,000 cells/well) and treated with varying concentrations of Imipramine Blue (0, 5µM in low serum HUVEC media) on the apical side of the transwell. Wells were filled with basal media to the level of media in the transwell, preventing a pressure gradient. Plates were incubated for 24 hours. Transwells were fixed with 4% paraformaldehyde, DAPI stained, and imaged under 20x to quantify invasion (%). Invasion percentages were normalized to the control (0µM) and

compared to the control using a student's two sample t-test (2 tail, α=0.05) to observe significant differences.

3.3. *IN VIVO* VASCULAR PERMEABILITY QUANTIFICATION

The *in vivo* vascular permeability study followed the timeline outlined in Table 1. .

Table 1: Treatment Groups for Vascular Permeability Study

Day	Treatment
0	Inoculate tumor
4	Tail vein injections Group 1, liposomal IB (n=3) Group 2, plain liposomes (n = 3)
7	Pre contrast images for random members of groups 1 and 2 Tail vein injections of dual gadolinium liposomes, both groups
10	MRI both groups
12	Perfusions

3.3.1. IMIPRAMINE BLUE LIPOSOME FORMULATION

Liposomes were synthesized by dissolving distearoyl (sn-glycero) phosphotidylcholine (DSPC) , poly (ethylene glycol) 2000- distearoyl-phosphatidyl ethanoloamine (DSPE-PEG2000), cholesterol, and 2 mg/ml Imipramine blue in ethanol. A molar ratio, 85:5:10, of DSPC: DSPE-PEG2000: cholesterol was dissolved in 10% final volume of ethanol at 70°C and hydrated with phosphate buffered saline (PBS) to 40 mM lipid molarity. The liposomes were then extruded five times through a 0.4 μm Nuclepore filter and then seven times through a 0.2μm Nuclepore filter using a 10ml Lipex Thermoline extruder to standardize the size of the liposomes to under 200 nm. The average diameter of the liposomes was determined using dynamic light scattering, which was approximately 160nm. Next, the remaining free drug was separated from the liposomes using a sepharose chromatography column. Finally, the solution was

diafiltrated to a smaller volume, approximately to a final IB concentration of 7 mg/ml in 140 mM lipids. IB concentration was quantified using a spectrophotometer with an excitation and emission of 590 nm and 625 nm. Prior to tail-vein injections, liposomes were filtered through a 0.2 μm pore filter.

3.3.2. PLAIN LIPOSOME FORMULATION

Liposomes were synthesized with a molar ratio, 85:5:10, of DSPC: DSPE-PEG2000: cholesterol, dissolved in 10% final volume of ethanol at 70°C, and hydrated with phosphate buffered saline (PBS) to 150 mM lipid molarity. The liposomes were then extruded five times through a 0.4 μm Nuclepore filter and then seven times through a 0.2μm Nuclepore filter using a 10ml Lipex Thermoline extruder to standardize the size of the liposomes to under 200 nm. The average diameter of the liposomes was determined using dynamic light scattering, which was approximately 160nm. The liposomes were dialyzed against PBS to remove the remaining ethanol. Prior to tail-vein injections, liposomes were filtered through a 0.2 μm pore filter.

3.3.3. DUAL GADOLINIUM LIPOSOME FORMULATION

Dual gadolinium liposomes were synthesized in a method similarly described by Ghaghada *et al.*[15] Liposomes were synthesized by dissolving DPPC, Gd-DTPA bis(stearylamide) (Gd-DTPA-BSA), cholesterol, and DSPE-PEG 2000 with a molar ratio of 30:25:40:5 in a chloroform-methanol (1:1 v/v) solution. The lipid solution was then evaporated to dryness using a vacuum and hydrated with a solution of gadodiamide (OmniScan®) to a final lipid concentration of 40mM. The solution was stirred at 60°C for 90 minutes. The liposomes were then extruded five times through a 400 nm Nuclepore membrane, seven times through a 200 nm Nuclepore membrane, and ten times

through a 100 nm Nuclepore membrane. The final liposome solution was then dialyzed against PBS to remove free gadolinium.

3.3.4. 3RT1-RT2A GLIOMA CELL CULTURE

The cell line was carried (trypsinized and washed with growth media) until the fourth passage, and 200,000 cells were suspended in 10 µl Leibovitz's L-15 Media.

3.3.5. TUMOR INOCULATION

Six Fisher 344 adult rats were implanted with tumors by sterile surgical techniques approved by the Institutional Animal Care and Use Committee (IACUC) at the Georgia Institute of Technology. The animals were anesthetized with 2-3% isoflurane and positioned in a stereotactic frame. The scalp was prepared and anesthetized with 0.5% marcaine. A 2-3 cm incision was made with a No. 10 scalpel. The periosteum was removed, and lambda was exposed. A 2 mm burr hole was drilled, 2 mm anterior and lateral from lambda. This injection point was determined to be common in glioma occurrences and yielded the most consistent tumors[17]. The 200,000 cells suspended in 10 µl Leibovitz's L-15 Media were slowly injected, 3 mm into the dura, using a Hamilton syringe. After injection, the syringe was slowly removed, and the burr hole was covered with bone wax. Finally, the scalp was sutured closed (Ethicon), and the rat was administered an intramuscular injection of buprenorphine (0.05mg/kg) to alleviate pain. Rats were monitored daily for signs of morbidity: change in fur color, weight loss, or inactivity.

3.3.6. TAIL VEIN INJECTIONS

On day 4 after tumor inoculations, the rats were administered tail-vein injections. Rats were randomly assigned to groups treated with either plain liposomes or Imipramine

Blue liposomes. Day 4 was chosen as the first day of injection because it is when angiogenesis is first seen in histological analysis. For the first treatment, groups were administered treatments (5mg IB/kg rat). On day 7, both groups were administered 0.15 mmol Gd/ kg rat.

3.3.7. MAGNETIC RESONANCE IMAGING

On day 7 prior to tail vein injections, one animal from each group was MR imaged for precontrast images. Animals were anesthetized by 1-2% Isoflurane, then placed in a 7T MRI (Bruker). A T1-weighted image was taken through the head using the following parameters: a range of 50ms - 2.0 s repetition time (TR), 48 ms echo time (TE), FOV = 40 mm x 40 mm with a 256 x 256 matrix, slice thickness = 5 mm, number of slices = 1, 4 averages per phase encode step requiring a total acquisition time of about 25 minutes per rat. Furthermore, a 3x3 cut out of a clear 96-well plate containing varying concentrations of dual-gadolinium liposomes were imaged.

3.3.8. IMAGE AND DATA ANALYSIS

3.3.8.1. KINETIC ANALYSIS

Vascular Permeability was assessed by determining each tumor's endothelial transfer coefficient (K^{PS} [ml min^{-1}100 cc^{-1} of tissue]) similarly to a method developed by Daldrup *et al*.[19] Concentration of gadolinium in the tumor (C_T) is a function of gadolinium accumulation in interstitial (C_I) and plasma spaces ($f_{pv}C_p$, where f_{pv} is the fractional plasma volume of the tumor tissue [mL cc^{-1} of tissue] and C_p is the concentration of gadolinium in the plasma [mmol ml^{-1}]) as seen in Eq. 1.

$$\mathbf{C_T(t) = C_I(t) + f_{pv}C_p(t)} \quad \textbf{(1)}$$

The rate of interstitial gadolinium accumulation (Eq. 2) is a function of the endothelial transfer coefficient (K^{PS}), the concentration of gadolinium in the plasma and the reflux from interstitial water back to the plasma, where k is the reflux rate constant.

$$\frac{\mathbf{dC_I(t)}}{\mathbf{dt}} = \mathbf{K^{PS}C_p(t) - kC_I(t)} \quad \textbf{(2)}$$

The solution to Eq. 2 is shown below in Eq. 3.

$$\mathbf{C_I = K^{PS}\int_0^t C_p(\theta)e^{-k(t-\theta)}d\theta} \quad \textbf{(3)}$$

Substituting C_I yields Eq. 4.

$$\mathbf{C_T(t) = K^{PS}\int_0^t C_p(\theta)e^{-k(t-\theta)}d\theta + f_{pv}C_p(t)} \quad \textbf{(4)}$$

3.3.8.2. MRI DATA EXTRACTION

Pre-contrast images were not used for the kinetic analysis of MR images because it was determined that the difference in tumor sizes from day 7 and day 10 would affect the amount of gadolinium accumulated at the tumor. MR images were converted into MATLAB colormaps by a program provided by Dr. Johannes Leisen. The colormaps displayed T_1 relaxivity and inverse T_1 relaxivity ($1/T_1$) values. T_1 and $1/T_1$ colormap scales were adjusted (T_1: (0, 4000); $1/T_1$: (4E-4, 8E-4)). Areas on the 96-well plate T1 colormap corresponding to varying concentrations of gadolinium were traced, and average RGB (red, green, blue) values were recorded. The RGB values were then

converted to T1 values on the colormap scale, and an exponential regression was created relating the amount of gadolinium (mmol) to T_1 values.

ImageJ was used for tumor analysis. Tumors on T_1 colormaps were outlined. Tumor area and mean tumor RGB values were extracted. RGB values were converted to T_1 values using the colormap scale. Finally, the T_1 values were converted to amounts of gadolinium (mmol) using the exponential regression. These values were divided by the product of the tumor area and MR image depth (volume of tumor section), converted to mmol/cc and recorded as C_T(t=72 hours).

No pharmacokinetics studies have been published for the dual gadolinium liposome formulation developed by Ghaghada *et al.,* so gadolinium accumulation in the plasma was modeled from a stealth liposome model.[15, 20] This model is analogous because of the similar lipid content. Stealth liposomes were core encapsulated with doxorubicin, and doxorubicin plasma levels were monitored over time[20]. Doxorubicin plasma concentration modeled a decreasing exponential curve (Figure 4). This model was applied to gadolinium accumulation. The vehicle of delivery (liposome) is what limits the amount of core encapsulated gadolinium which will be released into the plasma, so this is an applicable model for C_p(t). It was assumed that dual-gadolinium liposomes would have the same release profile in the plasma concentrations of mg/ml were converted to mmol/ml (Figure 5).

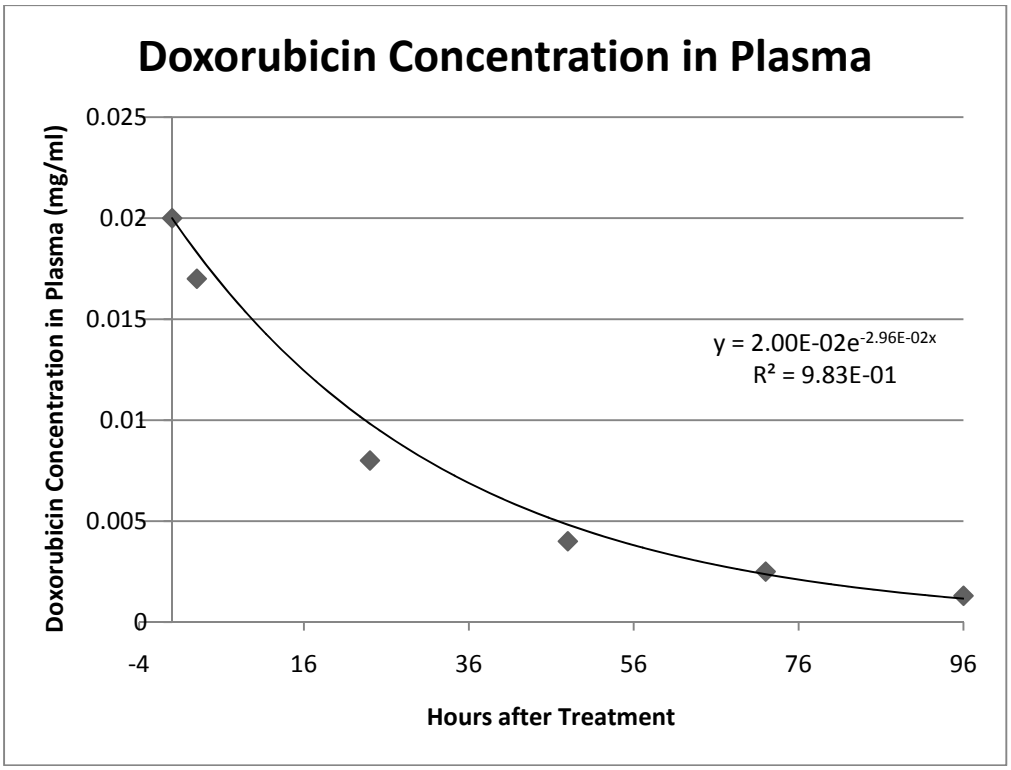

Figure 4: Doxorubicin concentration in plasma of rats treated with liposome-encapsulated doxorubicin.

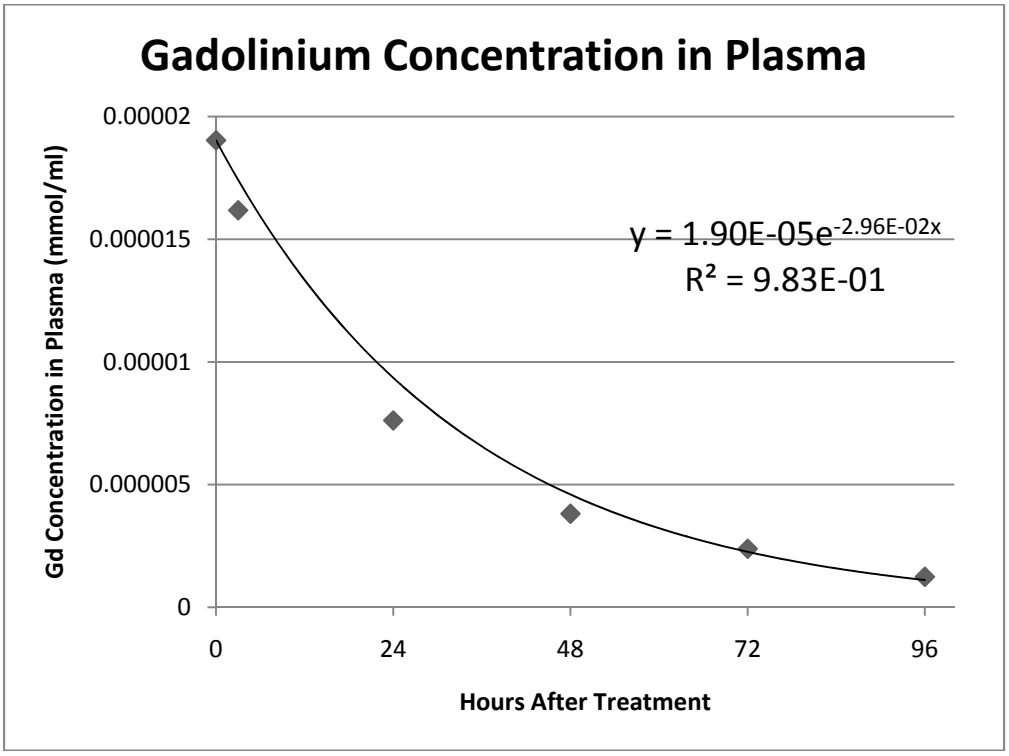

Figure 5: Predicted gadolinium concentration in plasma of rats treated with dual-gadolinium liposomes.

Daldrup *et al.* used k =0 for albumin-conjugated gadolinium.[19] Liposomes have a similar clearance rate as albumin, so k was also assumed to be 0 for the dual-gadolinium liposomes. Fractional plasma volume of 0.177 mL cc^{-1} was taken from control animals by a similar study by Gossman et al.[21] Rats were inoculated with U87 gliomas and MR imaged on day 16 to evaluate an anti-angiogenic therapy using the method described by Daldrup et al.[19] K^{PS} was then solved using Eq 4.

3.3.9. PERFUSIONS AND BRAIN PROCESSING

On day 12 the animals were perfused intracardially with PBS. Prior to perfusion, the rats were anesthethized by an intraperitoneal injection of ketamine, xylazine, and acetylpromazine (respectively 50, 10, and 1.67 mg/kg). Extracted brains were fixed in 4% paraformaldehyde in PBS for 1 hour at 4°C then stored in 4% sucrose (wt-vol % in PBS) at 4°C until saturated, embedded in optimal cutting temperature compound (OCT), stored at -80°C and cryosectioned coronally into 16 μm slices.

4. RESULTS

4.1. IN VITRO

4.1.1. MMP ACTIVITY

Some significant differences were observed in U87 and RT2A MMP activity (Figures 7 and 8). A significant difference was observed in U87 cells between 0.001 μM IB and 50 μM IB treatment groups(p=0.000). Similarly, significant differences were observed in RT2A cells between 1 μM IB and 50 μM IB (p=0.016). U87 MMP activity showed no definite increasing or decreasing trends as Imipramine Blue treatment

increased. As IB treatment increased, RT2A MMP activity increased from 0 µM IB to 0.1 µM IB and 1 µM IB, peaked, and then decreased from 1 µM IB to 100 µM IB.

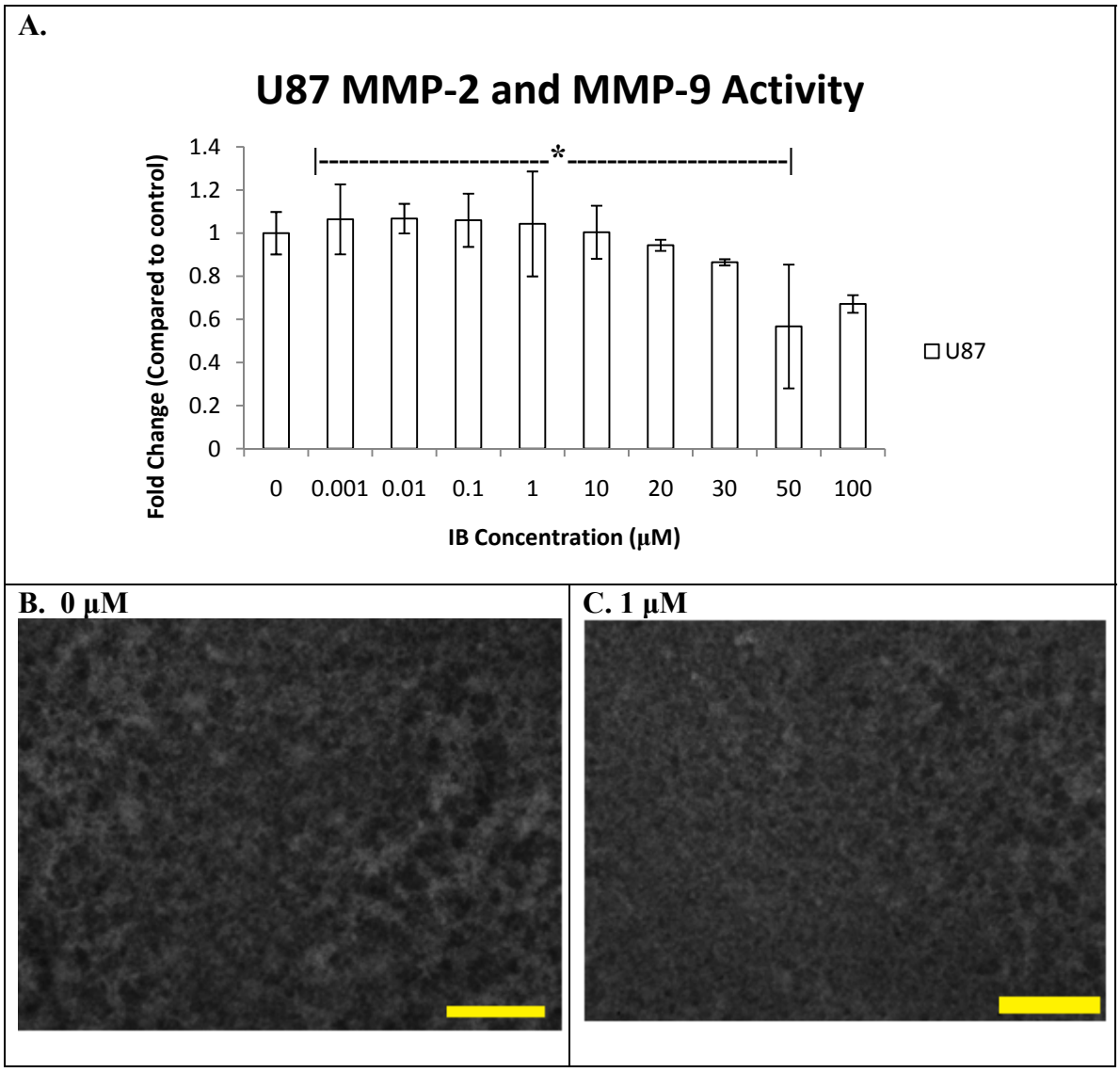

Figure 6: MMP Activity in IB-Treated U87 Cells. U87 cells were seeded on a basement membrane extract which included a dye-quenched collagen IV. When the collagen IV is cleaved by MMP-2 and MMP-9, a green fluoroscein is emitted. **A.** shows the treated U87 MMP-2 and MMP-9 activities. Asterixes denote the significant differences according to a one-way ANOVA and Tukey-post test (α=0.05). Significant differences were observed between treatment groups 0.001 µM IB and 50 µM IB (* p = 0.000),. **B.** and **C.**show the imaged wells at 10x for the 0 µM IB and 1 µM IB, respectively. Scale bar = 1cm.

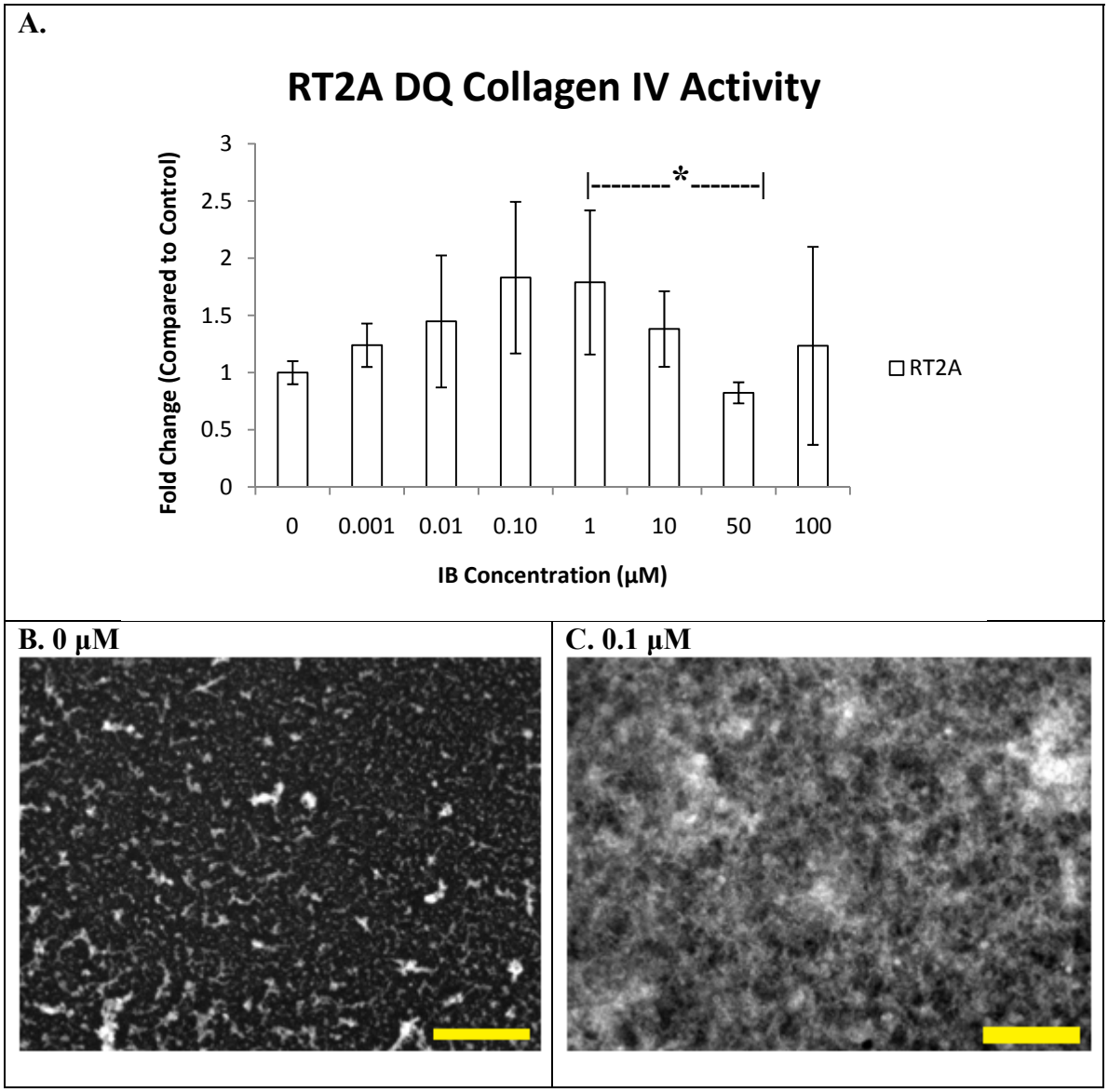

Figure 7: MMP Activity in IB-Treated RT2A cells. RT2A cells were seeded on a basement membrane extract which included a dye-quenched collagen IV. When the collagen IV is cleaved by MMP-2 and MMP-9, a green fluoroscein is emitted. **A.** shows the treated RT2A MMP-2 and MMP-9 activities. Asterixes denote significant differences according to a one-way ANOVA and Tukey-post test (α=0.05). Significant differences were observed between treatment groups 1 µM IB and 50 µM IB (* p = 0.016). **B.** and **C.**show the imaged wells at 10x for the control and 0.1µM IB, respectively. Scale bar = 1 cm.

4.1.2. HUVEC INVASION

Treated HUVEC invasion showed a decreasing trend but was not significant ($p = 0.08$, Figure 8).

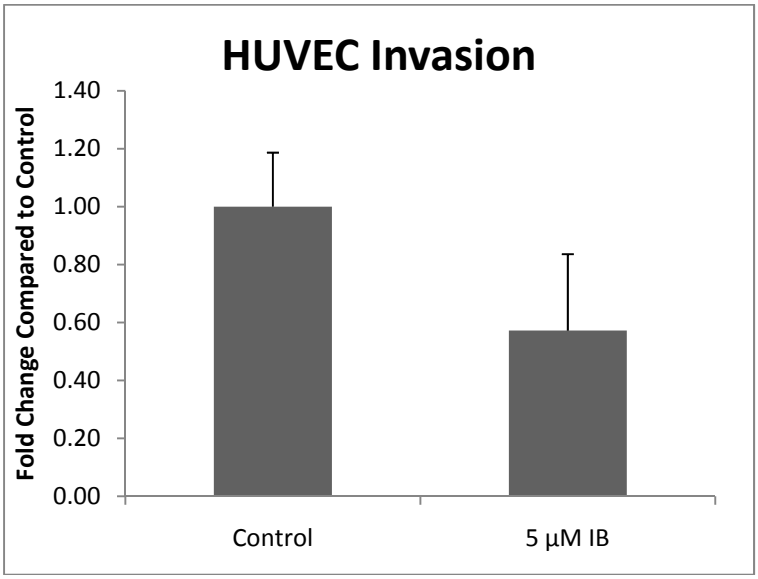

Figure 8: Invasion of IB-Treated HUVECs. HUVECs were seeded and treated either 0 µM IB or 5 µM IB (n=3 per treatment), incubated for 24 hours, 4% paraformaldehyde fixed, DAPI stained, and imaged. Invasion through the transwell was quantified and normalized to the control. Treated HUVEC invasion decreased but was not significant (2 sample t-test, 2 tail, $\alpha=0.05$,$p=0.08$).

4.2. *IN VIVO* VASCULAR PERMEABILITY QUANTIFICATION

No significant differences were observed between treatment groups in terms of endothelial transfer coefficients and cross-sectional tumor area ($p_1=0.3488$, $p_2=0.187$). MR images are seen in Figure 9, displaying the inverse T_1 relaxivities. Red areas indicate where gadolinium accumulated.

Table 2: Endothelial Transfer Coefficients (K^{PS}) and Cross-Sectional Tumor Areas in Plain Liposome-Treated and Imipramine Blue Liposome-Treated 3RT1-RT2A Tumors. Units for K^{PS} and cross sectional tumor area are mL $min^{-1}100\ cc^{-1}$ of tissue and mm^2. No significant differences were observed between treatment groups in terms of endothelial transfer coefficients and cross-sectional tumor area (p_1=0.3488, p_2=0.187).

Plain Liposomes			Imipramine Blue Liposomes		
ID #	K^{PS}	Cross-sectional tumor area	ID #	K^{PS}	Cross-sectional tumor area
1	0.647	0.808	4	13.466	0.058
2	6.927	0.126	5	3.398	0.209
3	0.908	0.576	6	3.907	0.248
Mean ± SD	2.83 ± 3.55	0.50 ± 0.35	Mean ± SD	6.92 ± 5.67	6.92 ± 0.10

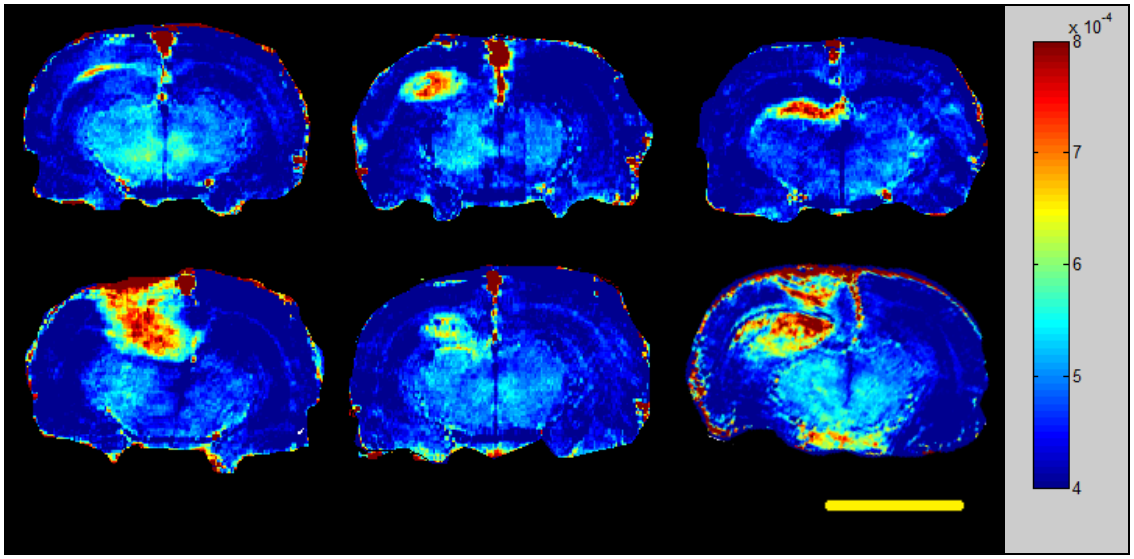

Figure 9: $1/T_1$ MR Brain Image Colormaps. Colormaps generated from MR data representing the inverse relaxivities. The red denotes the areas where gadolinium accumulated. Top row shows animals treated with plain liposomes (left to right: ID# 4-6). Bottom row shows animals treated with imipramine blue liposomes (left to right: ID# 1-3). Scale bar = 1cm.

5. DISCUSSION

MMP-2 and MMP-9 activity was not significantly affected by varying concentrations of Imipramine Blue. Although U87 and RT2A cells treated with 50 μM IB were significantly different from other treatment groups, it is expected that the significant decrease observed is due to cell death. From previous *in vitro* cytotoxicity assays, 40 μM IB was determined to be lethal for U87 and RT2A *in vitro*. This does not support the

prediction that Imipramine Blue affects basement membrane degradation, the first stage of angiogenesis. For future studies, it is suggested that positive control group be added, such as emodin, an MMP-2 and MMP-9 inhibitor observed in glioma cells.[22] The addition of a positive control group will confirm the appropriate sensitivity of the assay if no fluorescence is emitted. Zymography could also be performed for more quantitative results. Also, it is advised to look at other MMPs that could be involved in matrix degradation that are less commonly implicated in glioma since they still may be involved.

The HUVEC invasion assay showed a decreasing trend in endothelial cell migration when cells are treated with Imipramine Blue, but the results are not significant. Increasing the sample size by adding experiments for each treatment will provide more results. The assay performed only assesses the effect of IB on treated endothelial cells. Future experiments can simulate the effect of IB-treated glioma cells and their ability to recruit endothelial cells. This would involve glioma cells plated in a 24 well plate. Once adhered, cells would be treated with either 0 μM IB or 5 μM IB in basal media. Cells would be treated for 3 hours. *In vitro*, the effects of IB have been observed as early as 3 hours after treatment. After 3 hours of treatment, media will be replaced with low serum HUVEC media. Transwells containing seeded, untreated HUVECs using the method mentioned previously, will then be placed in the glioma-coated 24-well plate and incubated for 24 hours. Invasion through the membrane will be quantified using the same method previously mentioned. The addition of the coated glioma cell lines will simulate the tumor environment with the secretion of its chemokines during incubation.

No conclusions were made on the effect of Imipramine Blue on tube formation. Future experiments should include tube formation assays involving HUVECs treated with: varying concentrations of IB and a positive control tube formation inhibitor such as Avastin.[1] This will assess Imipramine Blue's possible abilities to prevent endothelial cell tube formation. The tube formation assay was not conducted with IB, but the Cultrex protocol was optimized with the use of low serum HUVEC media and 4% paraformaldehyde fixation to ensure proper tube formation prior to and after fixation.

In addition to no significant changes in MMP activity and HUVEC migration, no significant differences were observed between treatment groups in terms of endothelial transfer coefficients and cross-sectional tumor area, suggesting that IB does not affect vascular permeability. These results reject the alternative hypothesis that Imipramine Blue has an anti-angiogenic effect. In vivo, rats inoculated with the 3RT1-RT2A model were treated with saline or liposomal IB. Brains were dissected, sectioned, and stained for RECA-1 (rat endothelial cell antibody 1, a marker for blood vessels). RECA-1 staining showed that there were no significant differences in blood vessel amounts and cross-sectional areas between rats treated with plain liposomes and rats treated with IB liposomes; further suggesting that IB does not have an effect on angiogenesis.

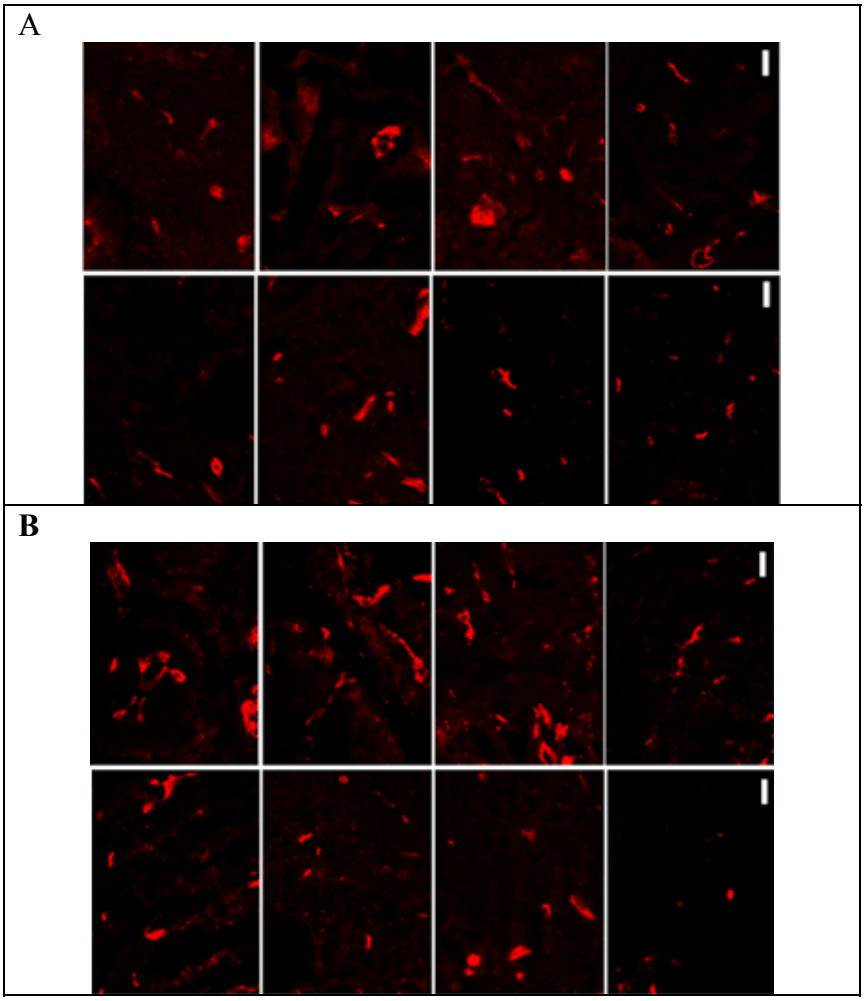

Figure 10: Effects of Imipramine Blue on Blood Vessels of Rat Gliomas (3RT1-RT2A). Rats were inoculated with gliomas and treated with either liposomal IB or saline. Brains were cryosectioned, stained for RECA-1, endothelial cell marker, and imaged along the border of the tumor. Rats treated with saline (A) appeared to have the same amount of blood vessels as rats treated with liposomal IB (B). Additionally, cross sectional areas of blood vessels did not vary between treatment groups. (Scale bar 50 microns)

The MRI method of determining vascular permeability is both novel and favorable because vascular permeability can be determined before perfusions, and the remaining dissected brain can be sectioned for histological analysis. Other methods for determining vascular permeability include Evans Blue quantification. This involves a tail vein injection prior to perfusions. After perfusions, the brain is dissected and the Evans Blue is extracted using a method described by Machein *et al*.[23] This method was practiced in a

pilot study, but no Evans Blue was extracted due to homogenizer problems. Therefore, determining vascular permeability from MR images is highly favored because it avoids extraction errors without the need of processing the brain after perfusions. Additionally, the use of dual-gadolinium liposomes increases circulation time allowing for a longer time frame for acquiring MR images but also decreases the necessary time for image acquisition due to the gadolinium's contrast agent properties.

A similar study was conducted comparing the effects of an anti-VEGF therapy on endothelial transfer coefficients in U87 inoculated tumors (400,000 cells in matrigel-media suspension per animal). Tumors were MR imaged on day 16. Given the cell amount inoculated and the additional amount of time to MR image, tumor sizes from the U87 study were larger. K^{PS} values were ten times greater in U87 PBS-treated tumors (control 28.6 ±8.6 mL $min^{-1}cc^{-1}$ of tissue, mean ±SD) compared to the 3RT1-RT2A plain liposome-treated tumors (control 2.83 ± 3.55 mL $min^{-1}cc^{-1}$ of tissue, mean ±SD), but this is most likely due to the difference in treatment timelines. Tumor size varied greatly within treatment groups, but this is probably due to the natural tumor size variability which depends on the individual animal. Increasing the sample size will likely lower the variability within tumor groups.

Many assumptions were made for this study, limiting the results. Fractional plasma volume constants were taken from the control animals in the study by Daldrup *et al*. The study's treatment groups had significantly different fractional plasma volume constants. If the treated Imipramine Blue animals did have a difference in vascular permeability, then estimating the fractional plasma volume to be the same could have eliminated a possible significant difference in endothelial transfer coefficients between treatment

groups. For future experiments, a better method for determining fractional plasma volume should be implemented. Additionally, a dual-gadolinium liposome pharmacokinetic study should be conducted to obtain a model for plasma gadolinium accumulation.

Despite the need for additional experiments, this method is still favorable for determining vascular permeability, and the addition of dual-gadolinium liposomes allows for longer circulation of contrast agent for longer image acquisition times and greater quality images. K^{PS} values were successfully determined from the MR images. Furthermore, this method allows for time point flexibility and post-perfusion analysis with the dissected brain.

6. CONCLUSION

MMP-2 and MMP-9 activity was not significantly affected by varying treatments of Imipramine Blue (within the viable concentrations). HUVECs treated with IB were not significantly affected. No conclusions were made in terms of tube formation, which should be investigated in future experiments. The newly developed method for determining vascular permeability *in vivo* is favorable and should be used for future studies because permeability data can be extracted prior to perfusion, and after perfusion, the extracted brain can be used for more analysis. Endothelial transfer coefficients were not significantly different between treatment groups. The lack of significant changes in MMP activity, endothelial cell recruitment, and endothelial transfer coefficients suggest Imipramine Blue has no anti-angiogenic effects, rejecting the alternative hypothesis that Imipramine Blue has anti-angiogenic properties.

7. REFERENCES

1. Norden AD, Young GS, Setayesh K, et al. Bevacizumab for recurrent malignant gliomas: efficacy, toxicity, and patterns of recurrence. *Neurology.* 2008;70(10):779-787.

2. Yamanaka R, Saya H. Molecularly targeted therapies for glioma. *Annals Of Neurology.* 2009;66(6):717-729.

3. Behin A, Hoang-Xuan K, Carpentier AF, Delattre J-Y. Primary brain tumours in adults. *The Lancet.* 2003;361(9354):323-331.

4. Vajkoczy P, Farhadi M, Gaumann A, et al. Microtumor growth initiates angiogenic sprouting with simultaneous expression of VEGF, VEGF receptor-2, and angiopoietin-2. *The Journal Of Clinical Investigation.* 2002;109(6):777-785.

5. Forsyth PA, Wong H, Laing TD, et al. Gelatinase-A (MMP-2), gelatinase-B (MMP-9) and membrane type matrix metalloproteinase-1 (MT1-MMP) are involved in different aspects of the pathophysiology of malignant gliomas. *British Journal Of Cancer.* 1999;79(11-12):1828-1835.

6. Cho K, Wang X, Nie S, Chen Z, Shin DM. Therapeutic Nanoparticles for Drug Delivery in Cancer. *Clinical Cancer Research.* March 1, 2008 2008;14(5):1310-1316.

7. Kim KY. Nanotechnology platforms and physiological challenges for cancer therapeutics. *Nanomedicine: Nanotechnology, Biology and Medicine.* 2007;3(2):103-110.

8. Jain RK, di Tomaso E, Duda DG, Loeffler JS, Sorensen AG, Batchelor TT. Angiogenesis in brain tumours. *Nat Rev Neurosci.* 2007;8(8):610-622.

9. Ceh B, Winterhalter M, Frederik PM, Vallner JJ, Lasic DD. Stealth® liposomes: from theory to product. *Advanced Drug Delivery Reviews.* 1997;24(2-3):165-177.

10. Schnyder A, Huwyler J. Drug Transport to Brain with Targeted Liposomes. *NeuroRX.* 2005;2(1):99-107.

11. Mukundan S, Jr., Ghaghada KB, Badea CT, et al. A liposomal nanoscale contrast agent for preclinical CT in mice. *AJR. American Journal Of Roentgenology.* 2006;186(2):300-307.

12. Ruoslahti E. Specialization of tumour vasculature. *Nature Reviews. Cancer.* 2002;2(2):83-90.

13. Immordino ML, Dosio F, Cattel L. Stealth liposomes: review of the basic science, rationale, and clinical applications, existing and potential. *Int. J. Nanomed.* 2006;1(3):297-315.

14. Gabizon A, Shmeeda H, Barenholz Y. Pharmacokinetics of pegylated liposomal Doxorubicin: review of animal and human studies. *Clinical Pharmacokinetics.* 2003;42(5):419-436.

15. Ghaghada KB, Ravoori M, Sabapathy D, Bankson J, Kundra V, Annapragada A. New Dual Mode Gadolinium Nanoparticle Contrast Agent for Magnetic Resonance Imaging. *PLoS ONE.* 2009;4(10):e7628.

16. OGAN MD, SCHMIEDL U, MOSELEY ME, GRODD W, PAAJANEN H, BRASCH RC. Albumin Labeled with Gd-DTPA: An Intravascular Contrast-Enhancing Agent for Magnetic Resonance Blood Pool Imaging: Preparation and Characterization. *Investigative Radiology.* 1987;22(8):665-671.

17. Munson J, McNeeley KM, De Hitta E, et al. Nanocarrier therapy for treating invasive glioma. *Society for Biomaterials*2009.
18. Sameni M, Cavallo-Medved D, Dosescu J, et al. Imaging and quantifying the dynamics of tumor-associated proteolysis. *Clinical and Experimental Metastasis.* 2009;26(4):299-309.
19. Daldrup H, Shames DM, Wendland M, et al. Correlation of dynamic contrast-enhanced magnetic resonance imaging with histologic tumor grade: comparison of macromolecular and small-molecular contrast media. *Pediatric Radiology.* 1998;28(2):67-78.
20. Woodle MC, Newman MS, Working PK. Biological Properties of Sterically Stabilized Liposomes. In: Lasic DD, Martin F, eds. *Stealth Liposomes*. Boca Raton: Taylor & Francis Inc; 1995.
21. Gossmann A, Helbich TH, Kuriyama N, et al. Dynamic contrast-enhanced magnetic resonance imaging as a surrogate marker of tumor response to anti-angiogenic therapy in a xenograft model of glioblastoma multiforme. *Journal of Magnetic Resonance Imaging.* 2002;15(3):233-240.
22. Kim MS, Park MJ, Kim SJ, et al. Emodin suppresses hyaluronic acid-induced MMP-9 secretion and invasion of glioma cells. *Int. J. Oncol.* Sep 2005;27(3):839-846.
23. Machein MR, Knedla A, Knoth R, Wagner S, Neuschl E, Plate KH. Angiopoietin-1 Promotes Tumor Angiogenesis in a Rat Glioma Model. *Am J Pathol.* November 1, 2004 2004;165(5):1557-1570.

8. ADDENDUM

Table 1: Treatment Groups for Vascular Permeability Study

Day	Treatment
0	Inoculate tumor
4	Tail vein injections Group 1, liposomal IB (n=3) Group 2, plain liposomes (n = 3)
7	Pre contrast images for random members of groups 1 and 2 Tail vein injections of dual gadolinium liposomes, both groups
10	MRI both groups
12	Perfusions

Table 2: Endothelial Transfer Coefficients (K^{PS}) and Cross-Sectional Tumor Areas in Plain Liposome-Treated and Imipramine Blue Liposome-Treated 3RT1-RT2A Tumors. Units for K^{PS} and cross sectional tumor area are mL min^{-1}100 cc^{-1} of tissue and mm^2. No significant differences were observed between treatment groups in terms of endothelial transfer coefficients and cross-sectional tumor area (p_1=0.3488, p_2=0.187).

Plain Liposomes			Imipramine Blue Liposomes		
ID #	K^{PS}	Cross-sectional tumor area	ID #	K^{PS}	Cross-sectional tumor area
1	0.647	0.808	4	13.466	0.058
2	6.927	0.126	5	3.398	0.209
3	0.908	0.576	6	3.907	0.248
Mean ± SD	2.83 ± 3.55	0.50 ± 0.35	Mean ± SD	6.92 ± 5.67	6.92 ± 0.10

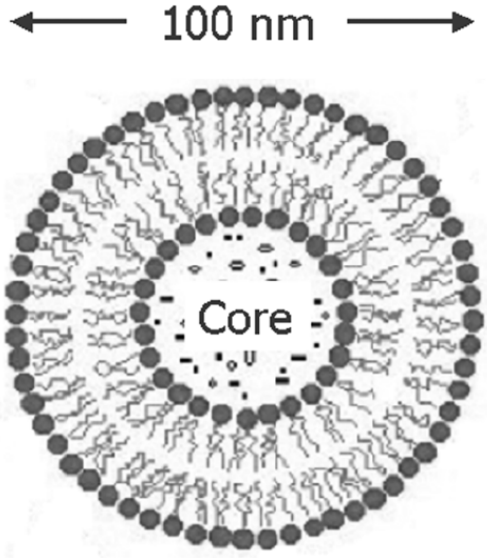

Figure 1: Liposome Schematic: Vesicle of about 100nm with a phospholipid bilayer and aqueous core.[11]

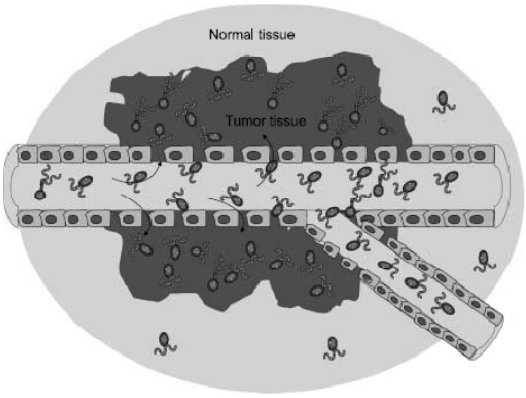

Figure 4: Nanoparticles delivered to tumor tissue via EPR Effect. The endothelial cells lining the blood vessel are more spaced out allowing nanoparticles of up to 400 nm in diameter to pass through and accumulate in a tumor.[6]

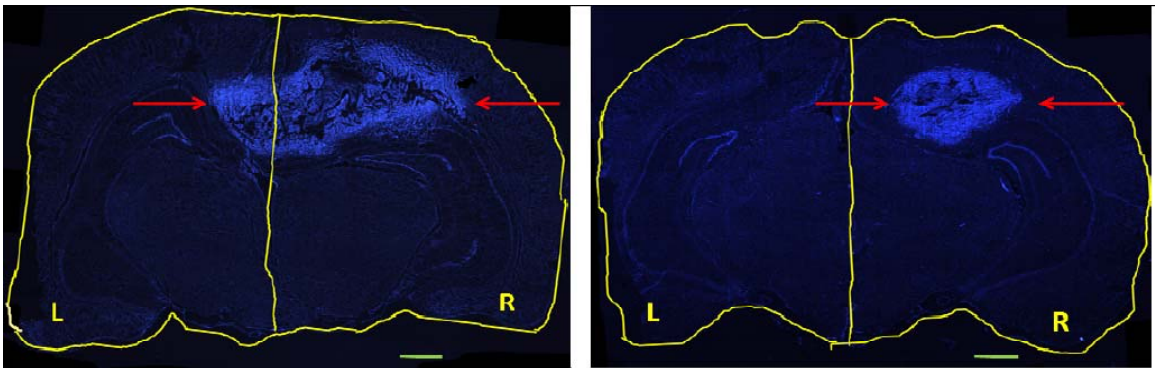

Figure 5: Effects of Imipramine Blue in Rat Glioma (3RT1-RT2A) Model. Tumors were injected 2mm anterior and lateral to lambda and 3 mm below the dura. Animals were administered tail-vein injections (saline or liposomal IB) on Day 4 and 7 (after tumor inoculation) and perfused on Day 11. Brains were sectioned coronally and stained with DAPI to highlight nuclei. The treated tumor appears more contained than the non-treated, suggesting IB's anti-invasive effects.[17]

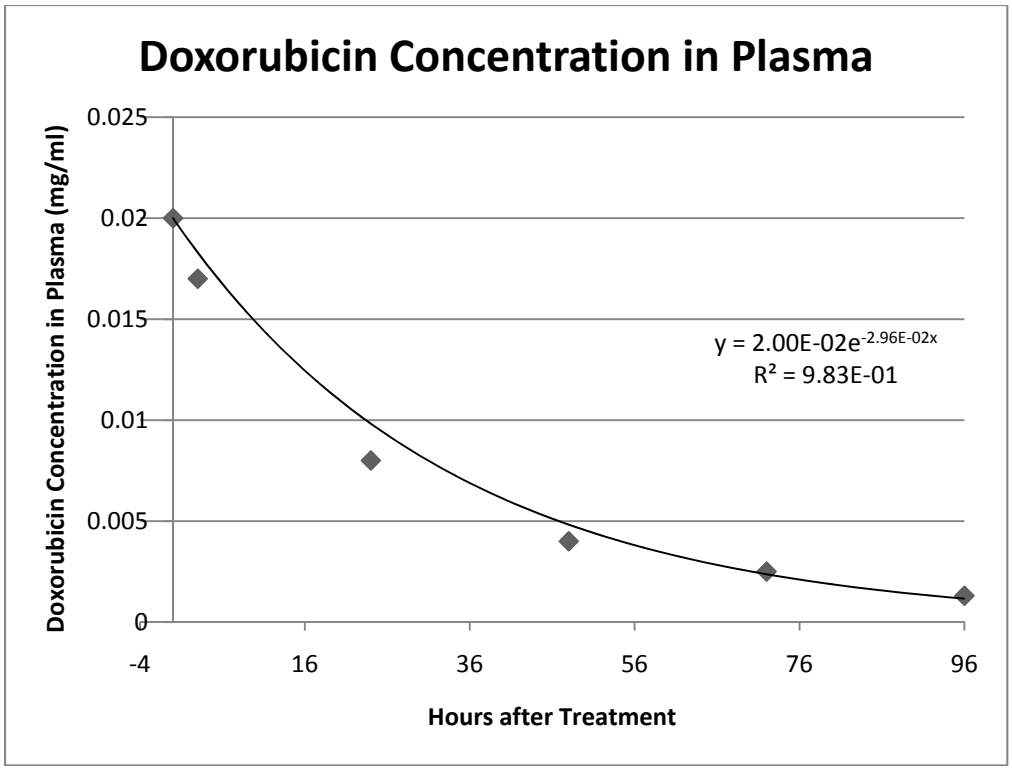

Figure 4: Doxorubicin concentration in plasma of rats treated with liposome-encapsulated doxorubicin.

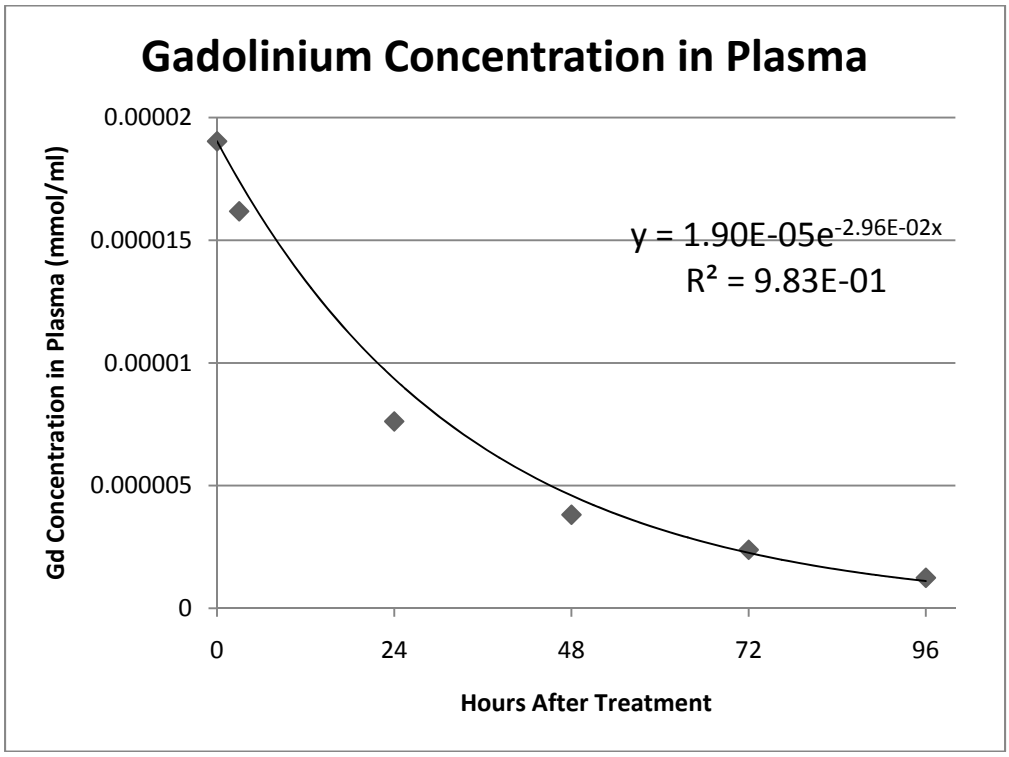

Figure 5: Predicted gadolinium concentration in plasma of rats treated with dual-gadolinium liposomes.

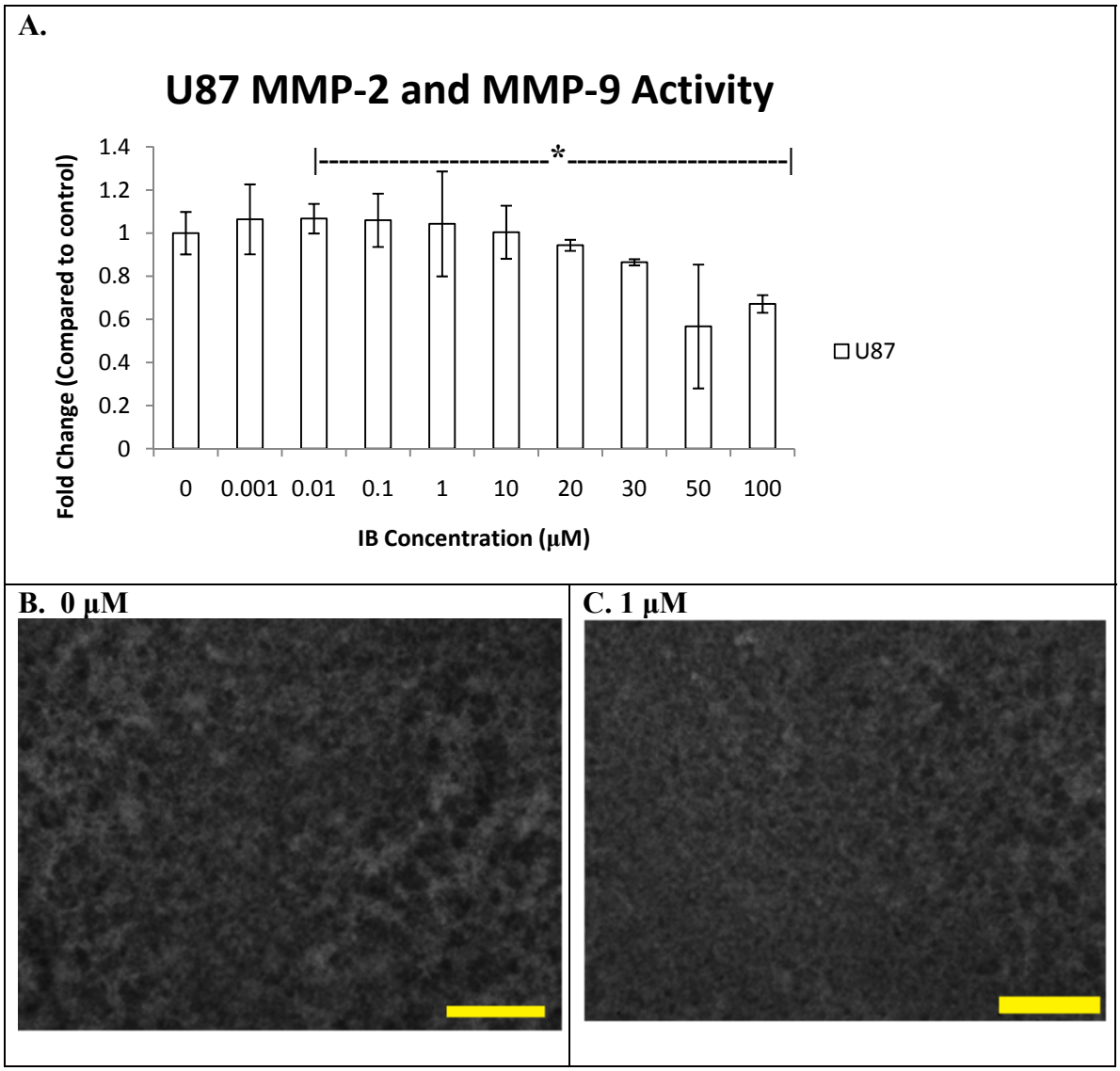

Figure 6: MMP Activity in IB-Treated U87 Cells. U87 cells were seeded on a basement membrane extract which included a dye-quenched collagen IV. When the collagen IV is cleaved by MMP-2 and MMP-9, a green fluoroscein is emitted. **A.** shows the treated U87 MMP-2 and MMP-9 activities. Asterixes denote the significant differences according to a one-way ANOVA and Tukey-post test (α=0.05). Significant differences were observed between treatment groups 0.001 µM IB and 50 µM IB (* $p = 0.000$),. **B.** and **C.**show the imaged wells at 10x for the 0 µM IB and 1 µM IB, respectively. Scale bar = 1cm.

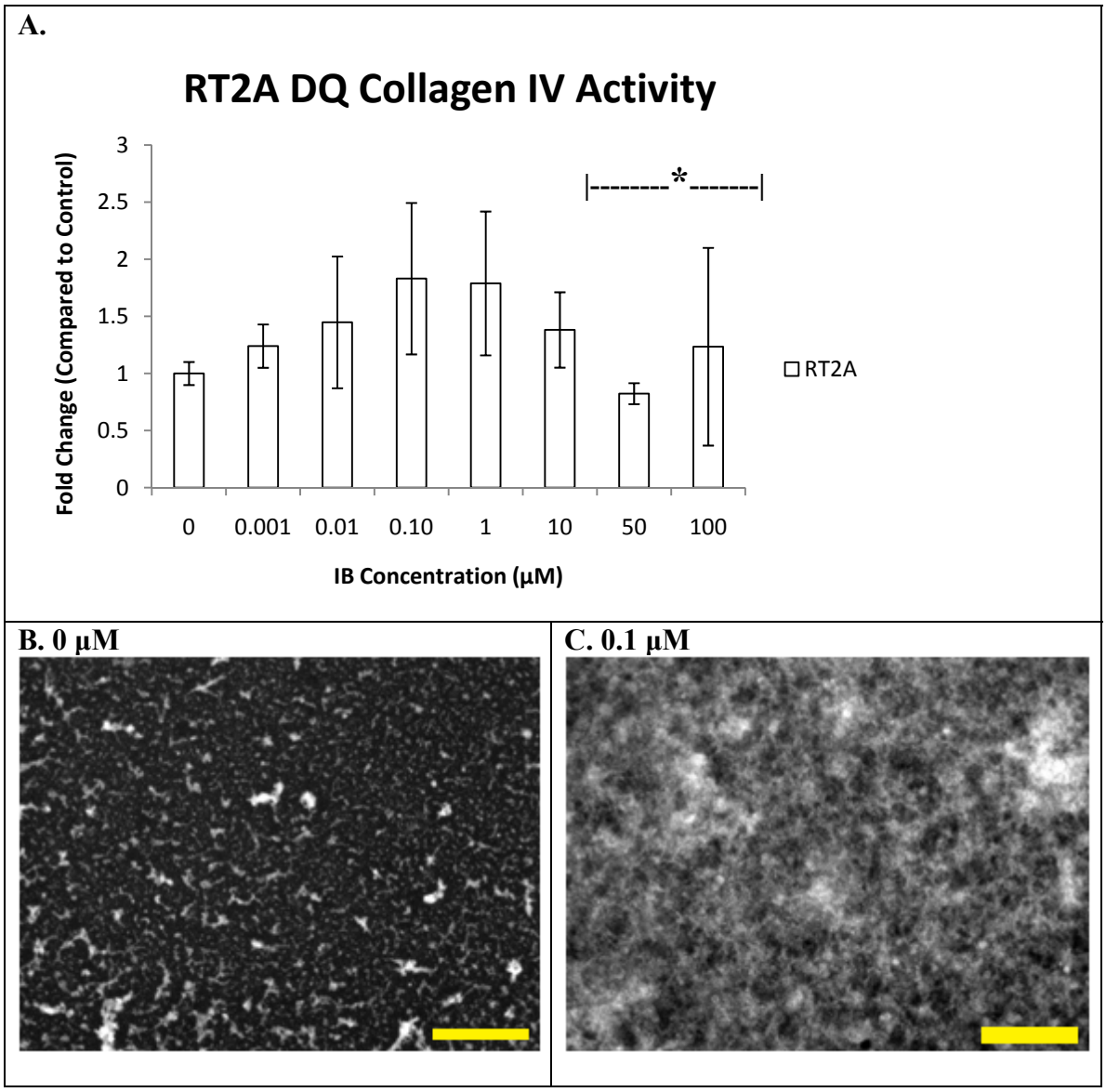

Figure 7: MMP Activity in IB-Treated RT2A cells. RT2A cells were seeded on a basement membrane extract which included a dye-quenched collagen IV. When the collagen IV is cleaved by MMP-2 and MMP-9, a green fluoroscein is emitted. **A.** shows the treated RT2A MMP-2 and MMP-9 activities. Asterixes denote significant differences according to a one-way ANOVA and Tukey-post test (α=0.05). Significant differences were observed between treatment groups 1 µM IB and 50 µM IB (* $p = 0.016$). **B.** and **C.**show the imaged wells at 10x for the control and 0.1µM IB, respectively. Scale bar = 1 cm.

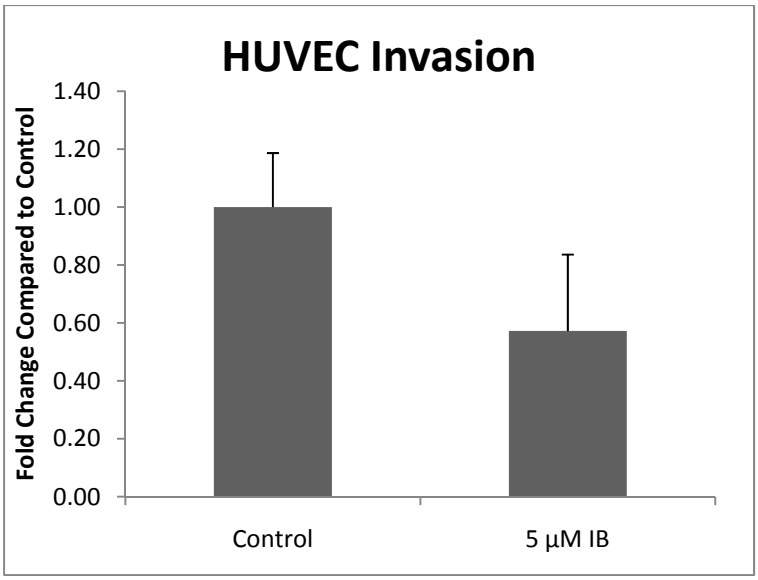

Figure 8: Invasion of IB-Treated HUVECs. HUVECs were seeded and treated either 0 µM IB or 5 µM IB (n=3 per treatment), incubated for 24 hours, 4% paraformaldehyde fixed, DAPI stained, and imaged. Invasion through the transwell was quantified and normalized to the control. Treated HUVEC invasion decreased but was not significant (2 sample t-test, 2 tail, α=0.05,p=0.08).

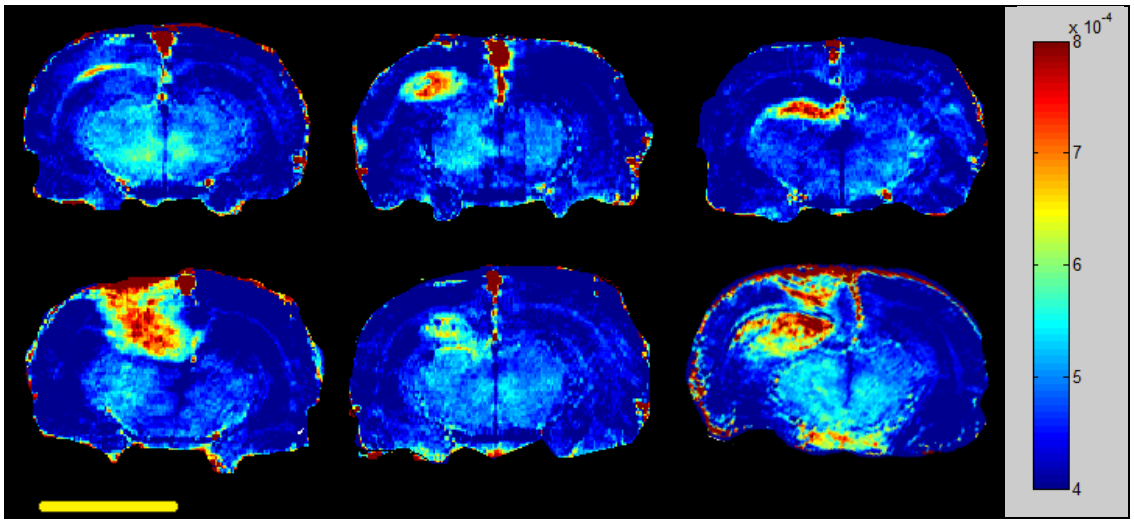

Figure 9: $1/T_1$ MR Brain Image Colormaps. Colormaps generated from MR data representing the inverse relaxivities. The red denotes the areas where gadolinium accumulated. Top row shows animals treated with plain liposomes (left to right: ID# 4-6). Bottom row shows animals treated with imipramine blue liposomes (left to right: ID# 1-3). Scale bar = 1cm.

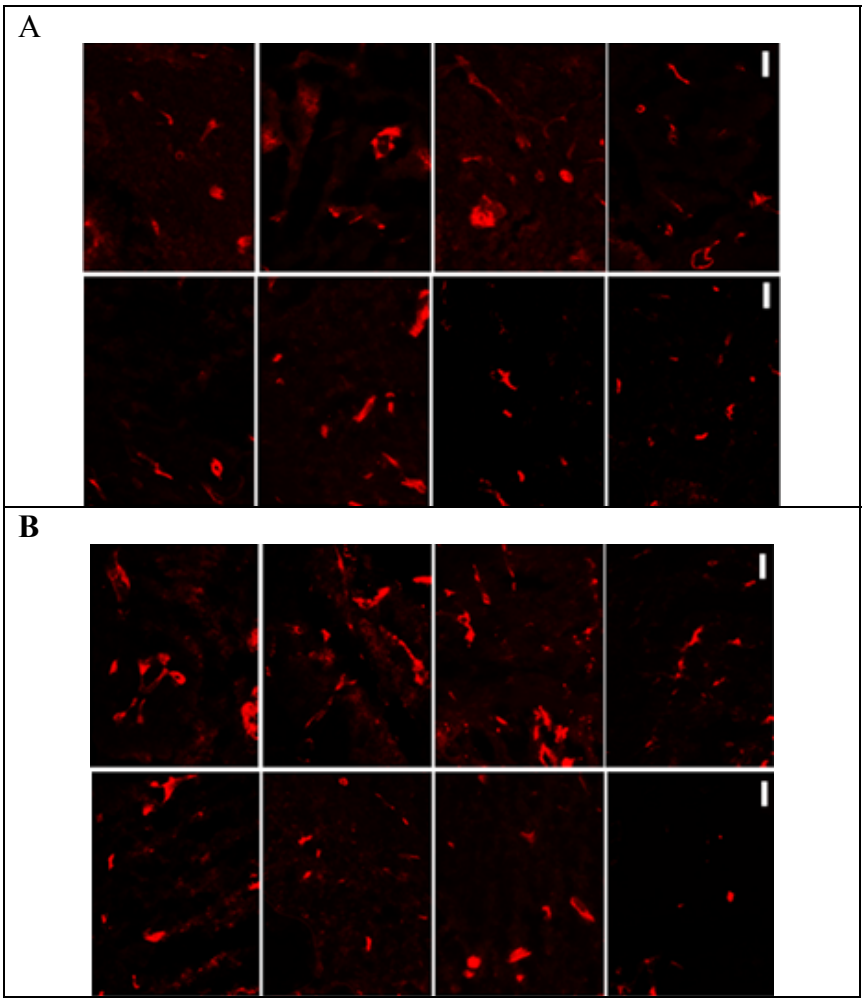

Figure 10: Effects of Imipramine Blue on Blood Vessels of Rat Gliomas (3RT1-RT2A). Rats were inoculated with gliomas and treated with either liposomal IB or saline. Brains were cryosectioned, stained for RECA-1, endothelial cell marker, and imaged along the border of the tumor. Rats treated with saline (A) appeared to have the same amount of blood vessels as rats treated with liposomal IB (B). Additionally, cross sectional areas of blood vessels did not vary between treatment groups. (Scale bar 50 microns)